Ocean-based Negative Emission Technologies

OCEAN NETs

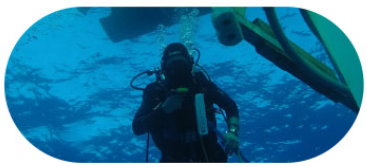

Deliverable Title	**D4.3 Analysis (report) of high- resolution modelling of efficacy, and regional impacts of selected ocean NETs close to the deployment sites**
Lead	GEOMAR
Related Work Package	WP 4
Related Task	Task 4.3
Author(s)	David P. Keller, Neha Mehendale, Tronje Kemena
Prieto Dissemination Level	Public
Due Submission Date	30.06.2023 (Interim report)
Actual Submission	03.11.2023
Project Number	869357
Start Date of Project	01. July 2020
Duration	60 months

Abstract: Many recent ocean modelling studies have demonstrated the added value of enhanced horizontal resolution, although it comes at a high computational cost. However, few modeling studies of ocean-based CDR have been done at high resolution. Here we assess the effects of model resolution on two simulated ocean-based CDR methods, unequilibrated ocean alkalinity enhancement (OAE) and the direct marine capture (DMC) of CO_2 from seawater (with assumed permanent storage), in experiments with the FOCI Earth system model. To do this we utilized two FOCI configurations, one with a 1/2° ocean resolution and the other with a 1/10° ocean nest in the N. Atlantic. Both configurations were run in a series of "paired" experiments with identical climate forcing and CDR deployments. We show that model resolution does appear to matter when simulating OAE and DMC. For OAE, parameterization of physical processes in the coarse resolution version of the model appears to overestimate how long alkalized waters stay in contact with the atmosphere and where they are transported. This results in large differences in OAE efficacy with almost twice as much carbon sequestered when the model resolution is coarse. For the DMC simulations, at one site there were clear differences in the compensating CO_2 flux induced by DIC removal, which was again higher with a coarse resolution, while at the other site variability was high and differences were difficult to determine. At both DMC sites there were clear differences in circulation with the two model resolutions, and thus on downstream biogeochemistry. We suggest that well resolving ocean physics may be necessary to best calculate unequilibrated OAE and DMC efficacies and side effects. These results should be confirmed using other models and with different resolutions.

This project has received funding from the European Union's Horizon 2020 research and innovation programme under grant agreement number 869357.

Document History

Date	Version	Description	Name/Affiliation
03.11.2023	1.0	Report	Keller (GEOMAR)

List of abbreviations, acronyms and definitions

NET Negative Emission Technologies
ESM Earth System Model
CDR Carbon Dioxide Removal
OAE Ocean Alkalinity Enhancement
FOCI Flexible Ocean and Climate Infrastructure climate model
TA Total Alkalinity
DIC Dissolved Inorganic Carbon
DMC Direct Marine Capture of CO_2 from seawater

List of figures

Figure 1. Schematic diagram of FOCI model components (from Matthes et al., 2020). The two main components (atmosphere and ocean) are coupled using OASIS3-MCT (Craig et al., 2017). Coupling occurs every three hours. The atmospheric chemistry component, HAMMOZ, is not used in this study.

Figure 2. Snapshot (5 d mean) of upper-ocean current speed at about 100 m depth, exemplifying the impact of the grid refinement, e.g., by allowing eddies to be resolved. The area covered by the two-way nested model VIKING10, in which the grid is refined from 1/2° to 1/10°, is marked by the red frame.

Figure 3. Schematic of the CDRMIP emission-driven SSP5-3.4-OS scenario experimental protocol (from Keller et al., 2018). A CO_2-emission- driven historical simulation is conducted until the year 2015. Then an emission-driven simulation with SSP5-3.4-OS scenario forcing is conducted. All experiments in this study end in the year 2100 or earlier.

Figure 4. Region of alkalinity addition (yellow) with the standard and nested grids. Note that in the nested configuration no alkalinity is added in the Mediterranean Sea (the yellow area here is an artifact of the plotting).

Figure 5. The boxes indicate the locations of where CO_2 is removed at a rate of 20.23 µmol kg^{-1} d^{-1} for the DMC experiments.

Figure 6. Comparison between observed GLODAP and simulated recent historical total alkalinity with both model versions.

Figure 7. Comparison between observed GLODAP and simulated recent historical dissolved inorganic carbon (DIC) with both model versions.

Figure 8. Simulated mean (years 2090 to 2100) total alkalinity (TA) increases with and without the nest (Nest and Standard respectively) for alkalinity added along the EU coast. Differences in the distribution of alkalinity towards the end of the simulations are shown in e, where the standard model output has been regridded to that of the nest for comparison.

Figure 9. Simulated global annual mean oceanic CO_2 uptake (Pg C yr^{-1}) for both model configurations with and without (referred to as control run or baseline) OAE.

Figure 10. Simulated mean (years 2090 to 2100) changes in ocean CO_2 uptake due to OAE for the standard (a) and nested (b) model configurations. Differences (Nest – Standard) between the model versions are shown in (c). All data is shown on the standard grid.

Figure 11. Simulated changes in oceanic dissolved inorganic carbon (DIC) with and without the nest (Nest and Standard respectively) for the baseline(control) and OEA experiments (a and b) and the difference between the OAE and baseline experiments (e), i.e., carbon sequestered and stored due to OAE. In (e) the cumulative difference in DIC at the year 2100 is noted. In (c) and (d) mean (years 2090 to 2100) water column inventory DIC changes are shown, with differences between the model configurations shown in (f), where the standard model output has been regridded to that of the nest for comparison.

Figure 12. The global total change in alkalinity or DIC (a) and the efficacy of OAE at increasing oceanic carbon storage (b) when calculated as the global change in DIC per change in alkalinity. All differences (deltas) are relative to the baseline (control) run simulations for both model resolution configurations. In (b) years during the OAE ramp-up phase are not shown due to internal model variability that produce a large range of efficiencies.

Figure 13. Simulated mean (years 2090 to 2100) changes in ocean pH for the standard (a) and nested (b) model configurations during OAE. Differences (Nest – Standard) between the model versions are shown in (c).

Figure 14. Surface grid cell dissolved inorganic carbon (DIC) and the change in DIC (DMC – baseline run) at the direct marine capture (DMC) sites in the North Sea and off the coast of Spain. Only DMC simulations are shown. The vertical grey dashed line indicates the date at which DMC was stopped in the DMC experiments.

Figure 15. Simulated surface ocean DIC for the standard (a) and nested (b) model configurations on Jan. 25, 2025 during DMC. Differences (Nest – Standard) between the model versions are shown in (c). The extreme values near the coastline in (a) and (c) are the result of re-gridding the coarse resolution (0.5°) output onto the high-resolution grid for comparison and represent areas where there is no output due to the lower resolution.

Figure 16. Snapshot of the daily mean change in the surface ocean CO_2 flux for the standard (a) and nested (b) configurations, relative to their baseline (control) simulations, after 25 days of Direct Marine Capture (DMC) of DIC. The CO_2 flux difference between the nested and standard DMC experiments is shown in (c) where the standard model output has been re-gridded to that of the nest for comparison.

Figure 17. Simulated CO_2 fluxes at the direct marine capture (DMC) sites in the North Sea (a and c) and off the coast of Spain (b and d) with both model resolution configurations and for baseline and DMC experiments. Cumulative carbon uptake, calculated from the CO_2 flux data is shown in (c) and (d). The vertical grey dashed line indicates the date at which DMC was stopped in the DMC experiments.

Figure 18. Surface ocean pH for the at the DMC removal sites.

Figure 19. Snapshot of the daily mean change in surface ocean pH for the standard (a) and nested (b) configurations, relative to their baseline (control) simulations, after 25 days of Direct Marine Capture (DMC) of DIC. The pH difference between the nested and standard DMC experiments is shown in (c) where the standard model output has been re-gridded to that of the nest for comparison.

1. Introduction

1.1 Context

OceanNETs is a European Union project funded by the Commission's Horizon 2020 program under the topic of Negative emissions and land-use based mitigation assessment (LC-CLA-02-2019), and coordinated by GEOMAR | Helmholtz Center for Ocean Research Kiel (GEOMAR), Germany.

OceanNETs responds to the societal need to rapidly provide a scientifically rigorous and comprehensive assessment of negative emission technologies (NETs). The project focuses on analyzing and quantifying the environmental, social, and political feasibility and impacts of ocean-based NETs. OceanNETs will close fundamental knowledge gaps on specific ocean-based NETs and provide more in-depth investigations of NETs that have already been suggested to have a high CDR potential, levels of sustainability, or potential co-benefits. It will identify to what extent, and how, ocean-based NETs can play a role in keeping climate change within the limits set by the Paris Agreement.

1.2 Purpose and scope of the deliverable

This deliverable is a product of Task 4.3: *Understanding the role of model resolution in simulated NET outcomes.* In this task the aim was to assess the effects of model resolution on the simulated efficacy of CDR methods. To do this the FOCI Earth system model was run with and without high resolution (a few kilometers grid scale) nesting to assess effects of either explicitly resolving some physical processes such as ocean eddies or implicitly resolving them via a parameterization. The high-resolution nest was placed over future potential ocean CDR deployment sites in the EU as partially determined by the WP6 case studies. However, due to the timing of the development of the case studies the nature of the deployment is idealized (i.e., we had to start these simulations before the case study information was fully developed). Nonetheless, the results help to guide the interpretation of modelling experiments of ocean NETs done with coarser resolution ESMs in other WP4 tasks. They also provide information on whether or not one should use much more computationally expensive high-resolution models when investigating certain aspects of ocean-based CDR approaches.

1.3 Relation to other deliverables

As mentioned above the results of this study can be used to guide the interpretation of modelling experiments of ocean NETs done with coarser resolution ESMs in other WP4 tasks. However, no other tasks or deliverables directly depend on the results of this study.

2. Technical part of the deliverable

2.1 Introduction

Modelling studies have played a key role in investigating ocean-based carbon dioxide removal (CDR). Much of the early work on ocean-based CDR was been done through idealized modeling approaches with coarse resolution (≥ 1°) Earth system models (ESMs), often of intermediate complexity. These experiments were designed to investigate if the theoretical concept of CDR would work to remove large amounts of CO_2 when scaled up. This meant that rather than trying

to account for "realistic" technical and socio-economic constraints of CDR deployment, the experiments investigated what would happen if CDR was done at a large scale. For this purpose, the models also did not need to be too detailed or complex, but only to be able to simulate key aspects of the Earth system, e.g., the models need not simulate interannual variability, only the general climate. The results of these experiments were then able to suggest if the approach is viable. A particular advantage of this idealized approach is that the effect of CDR is often easy to detect against internal model variability, i.e., the signal to noise ratio is high. The next steps in modelling CDR have remained idealized, but begin to introduce more constraints and better mechanistic or empirically derived components as experimental CDR data becomes available that continue to shift toward a more realistic way of modeling CDR. Very recently modeling has started to be tailored to support experiments, field trials or commercial deployments. These applications of course have to be as realistic as possible. One of the major uncertainties in all of this modeling work is how well the models actually simulate the CDR approach. There are many aspects that have to be considered when answering this question. Here we focus on one particular topic, model resolution and the role that it plays in being able to explicitly resolve physical processes vs. having to parameterize them.

Many recent studies with global ESMs have demonstrated the added value of enhanced horizontal resolution (Haarsma et al., 2016). In the ocean these include improved simulation of boundary currents, water exchange through narrow straits, coastal currents, upwelling, oceanic eddies, fronts and other physical features. For some ocean-based CDR approaches such as ocean alkalinity enhancement (OAE) or the direct removal of CO_2 from seawater, the simulation of these physical features is of particular importance because they play an important role in air-sea gas exchange dynamics. For unequilibrated OAE, the longer that the water to which alkalinity has been increased in, remains at the surface the more time it has to equilibrate with the atmosphere, thereby controlling the short-term efficacy of OAE. For example, if OAE is done in a region where the higher alkalinity water is subducted into the deep ocean before full equilibration, then the efficacy will be lower than for OAE done in a region where the water mass can fully equilibrate with the atmosphere. It is only after the subducted water again comes into the atmosphere that equilibration could then occur, something that could take hundreds to thousands of years, thereby delaying CDR. Since most ocean-based CDR studies have been conducted with fairly coarse resolution models that parameterize mesoscale and sub-mesoscale processes it remains to be seen if these models accurately represent critical physical processes controlling efficacy.

In this study we use an ESM called FOCI, which has the capability to be run with and without high resolution regional nests, to investigate if changes horizontal model resolution affects the simulation of ocean-based CDR. To do this we utilized two FOCI configurations, one with a 1/2° ocean resolution and the other with a 1/10° ocean nest in the North Atlantic. Both configurations were run in a series of "paired" experiments with identical climate forcing and CDR deployments. We hypothesize that for ocean-based CDR approaches such as OAE or direct CO_2 removal from surface seawater, the explicit resolution of physical features such as eddies and fronts will reduce the near-term efficacy of the approach.

2.2 Methodology

2.2.1 Model Description

The model used in this study is the Flexible Ocean and Climate Infrastructure (FOCI) climate model (Matthes et al., 2020), which supports the coupling of independent model components in a flexible manner (Fig. 1). The main components include a general circulation model of the

atmosphere and of the ocean together with a coupler. Additional components include land, sea-ice, atmospheric chemistry and marine biogeochemistry (Chien et al., 2022).

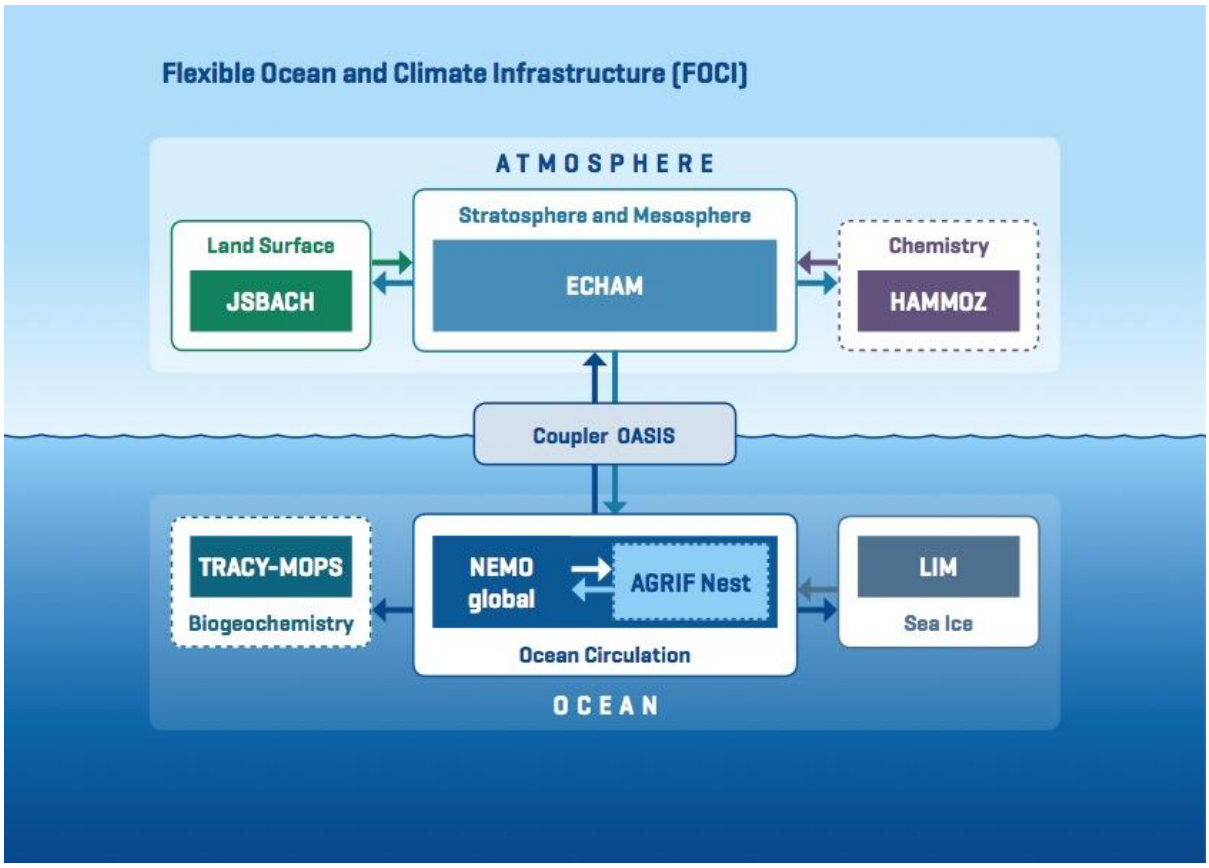

Figure 4. Schematic diagram of FOCI model components (from Matthes et al., 2020). The two main components (atmosphere and ocean) are coupled using OASIS3-MCT (Craig et al., 2017). Coupling occurs every three hours. The atmospheric chemistry component, HAMMOZ, is not used in this study.

The atmosphere within FOCI is modelled by the ECHAM (European Center HAMburg) model version 6.3. ECHAM is coupled to the land surface model JSBACH v. 3 (Schneck et al., 2013). Both models have been developed at the Max Planck Institute for Meteorology. Atmosphere resolution in FOCI is T63L95, corresponding to a horizontal resolution of 1.8° and 95 vertical levels, including the stratosphere. The optional atmospheric chemistry module HAMMOZ is not used in this study.

The ocean is modelled using the ocean general circulation model Nucleus for European Modelling of the Ocean (NEMO) version 3.6 (Madec, 2016). The standard FOCI configuration employs the ORCA05 grid (a tripolar grid at 1/2° nominal horizontal resolution) with 46 vertical layers, that is coupled to the LIM2 sea-ice model (Louvain-la-neuve Ice Model; Madec 2016). Within the ocean, FOCI has the capability to integrate AGRIF nests (Fig. 2), which enhance the horizontal resolution over specific regions from 1/2° to 1/10°. In this study we use both configurations, the standard 1/2° one, and a version with the VIKING10 North Atlantic nest, which is between 30° and 85° N (Fig. 2).

A marine biogeochemistry model, MOPS (Model of Oceanic Pelagic Stoichiometry), that resolves C, N, P, and O_2 cycling, is implemented within FOCI (Chien et al., 2022). MOPS simulates the cycling of nutrients (phosphate and nitrate), phytoplankton, zooplankton, detritus, and dissolved organic matter (I Kriest & Oschlies, 2015). Biogeochemical parameters have been optimized to fit against global climatologies of observed macronutrients and oxygen (Iris Kriest et

al., 2017). The description of air-sea oxygen gas exchange in TRACY-MOPS is based on Orr et al. (2017) and the carbonate chemistry description is based on Orr and Epitalon (2015) with the difference that carbonate system variables (e.g. pH, pCO_2) are only computed for the ocean surface layer (and not in the ocean interior) and therefore pressure corrections are not included in the model code. The biogeochemical model also includes a simple module for calcite production, export, and dissolution following Schmittner et al. (2008), and is calibrated against global climatologies of DIC and alkalinity.

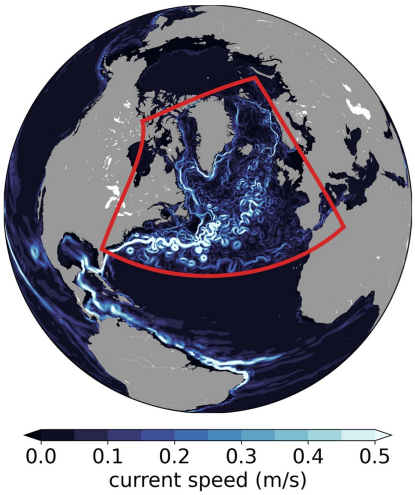

Figure 5. From Martin and Biastoch, (2023). Snapshot (5 d mean) of upper-ocean current speed at about 100 m depth, exemplifying the impact of the grid refinement, e.g., by allowing eddies to be resolved. The area covered by the two-way nested model VIKING10, in which the grid is refined from 1/2° to 1/10°, is marked by the red frame.

2.2.2 Experimental Design

To investigate the importance of model resolution when simulating ocean-based CDR we utilized two FOCI configurations, one with the standard 1/2° ORCA05 ocean resolution and the other with the 1/10° VIKING10 ocean nest in the N. Atlantic. Hereafter, these configurations will be referred to as "standard" (1/2° resolution) and "nested" (1/10° resolution). Both configurations were run in a series of "paired" experiments (described below) with identical climate forcing and CDR deployments. All simulations were run in "ESM" mode as described in the C4MIP protocol (Jones et al., 2016) with CO_2 emissions being prescribed and atmospheric CO_2 as a prognostic variable. The CDR experiments were not run for an extended period of time, e.g., beyond the year 2100 for the OAE runs, due to the computational expense of performing simulations with the nested version of the model.

Climate forcing: In all experiments, ScenarioMIP SSP5-3.4-OS scenario (O'Neill et al., 2016) forcing is used following CDRMIP protocols (Keller et al., 2018) until the year 2100 (the long-term extension was not simulated). This scenario prescribes atmospheric CO_2 emissions to follow an overshoot pathway of high emissions until 2040, that is followed by aggressive mitigation to reduce emissions to zero by about 2070, with substantial negative global emissions (i.e., CO_2 removal) thereafter (Fig. 3). To do this we first performed the CMIP6 emission driven historical simulation, *esm-hist*. Then using this as a starting point, conducted emission-driven SSP5-3.4-OS scenario simulations, *esm-ssp534-over*, (starting on January 1, 2015). All non-CO_2 forcing (e.g., land use) is identical to that in the ScenarioMIP *ssp534-over* simulations. Hereafter, we refer to the SSP5-3.4-OS simulations without CDR as the baseline or control simulation, which is used for comparative purposes, i.e., to detect a change due to CDR.

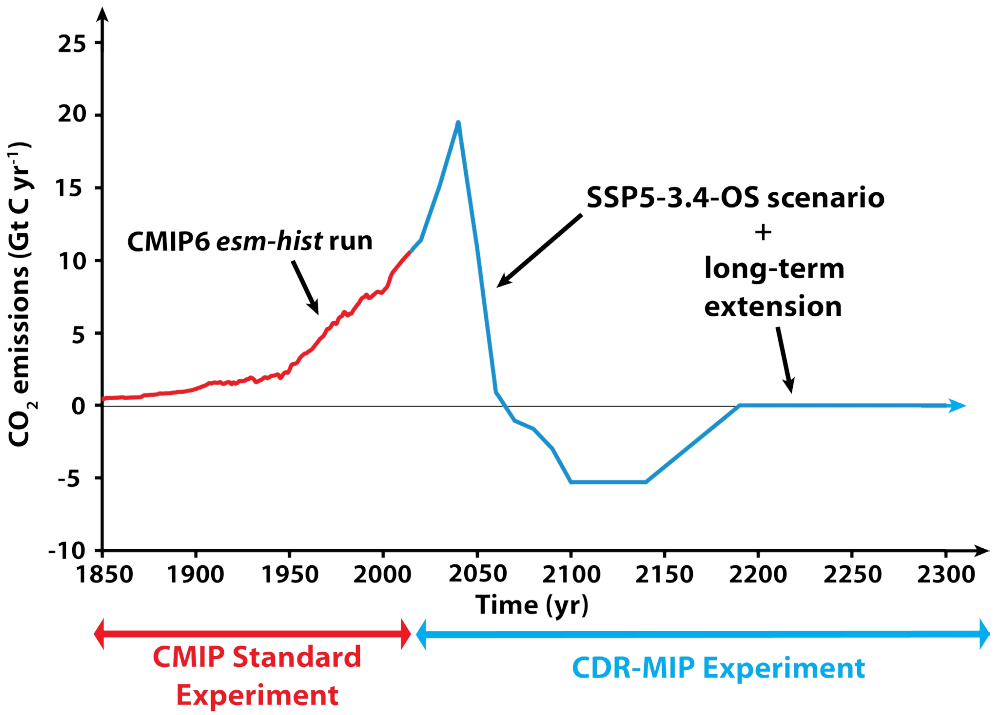

Figure 6. Schematic of the CDRMIP emission-driven SSP5-3.4-OS scenario experimental protocol (from Keller et al., 2018). A CO_2-emission- driven historical simulation is conducted until the year 2015. Then an emission-driven simulation with SSP5-3.4-OS scenario forcing is conducted. All experiments in this study end in the year 2100 or earlier.

Ocean alkalinity enhancement experiments: Ocean alkalinity enhancement (OAE) is simulated along the European coastline within an ~50 km region (Fig. 4), excluding the Baltic and Mediterranean Sea as these are not fully included in the VIKING10 nest (Fig. 2). OAE was done in the same area with and without the nest, which means that OAE covered 5 grid cells in the nested version to equal one grid cell in the standard version. However, as OAE was coastally deployed this meant that in the nest there were sometimes features like bays that were not present in the standard version due to the resolution. With both resolutions, the simulated addition of $Ca(OH)_2$ begins in the year 2025 with the rate of addition linearly increasing over 10 years until ~1 Gt $Ca(OH)_2$ is being added from the year 2035 onward. Note that in practice simulating OAE is done via a flux of total alkalinity (TA) into the upper (surface) model grid cells as the model does not have explicit tracers for $Ca(OH)_2$. Due to numerical issues (e.g., losses during the calculated advection of the tracers) slightly different amounts OAE were simulated in the two model configurations with cumulative year 2099 TA changes of 0.9633283 and 0.97282311 Pmol in the standard and nest versions, respectively. Model output was written as monthly means for most variables.

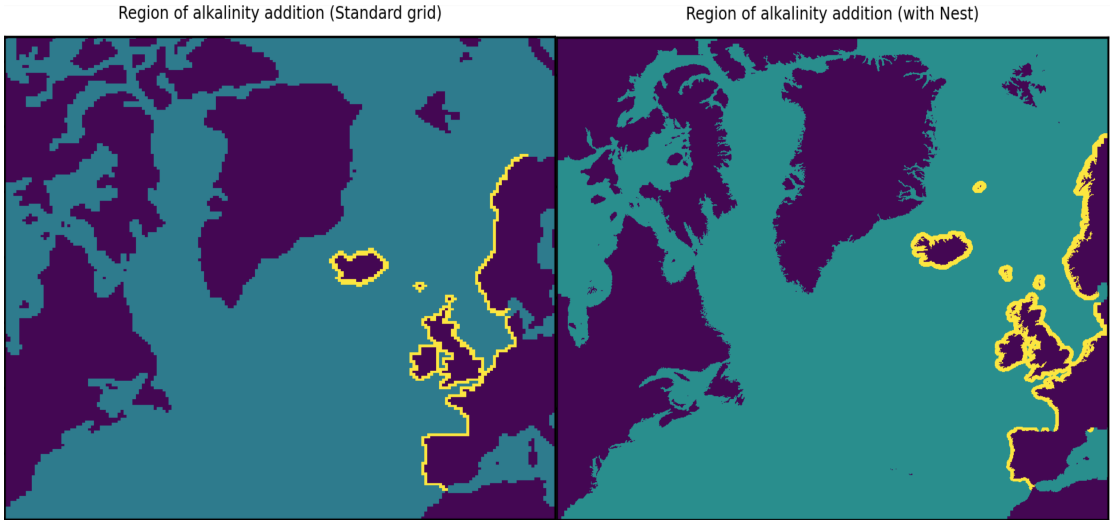

Figure 4. Region of alkalinity addition (yellow) with the standard and nested grids. Note that in the nested configuration no alkalinity is added in the Mediterranean Sea (the yellow area here is an artifact of the plotting).

Direct CO_2 removal from seawater experiments: Direct Marine Capture (DMC) of CO_2 is simulated in two regions. One is in the North Sea and the other in the Atlantic upwelling region off the Iberian Peninsula (Fig. 5). The selected area is the same with both model resolutions, but of course with more grid cells included in the nested version to equal the same area in each standard resolution grid cell. The rate of removal is idealized as current DMC technology is immature and upper scaling limits per unit area are unknown (NAESM 2021). Removal was thus calculated by determining what 30% of total DIC at the points were on Jan. 1, 2025 and then removing this amount daily, which corresponds to a DMC DIC removal rate of 20.23 µmol kg^{-1} d^{-1}. DMC was done at each location for 1 month (Jan. 2025), followed by a month (Feb. 2025) without removal. Model output was written as daily means. The removed carbon is assumed to be stored permanently, e.g., in a geological formation.

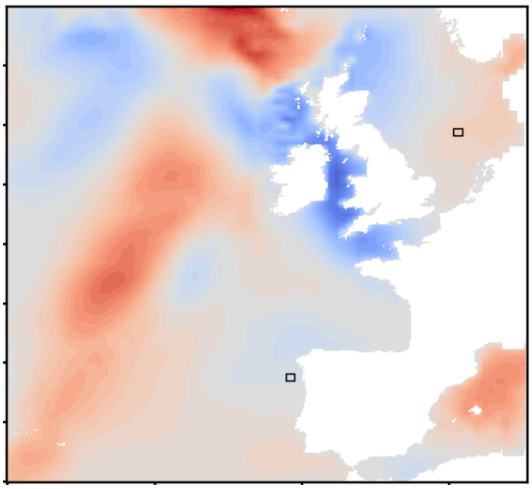

Figure 5. The boxes indicate the locations of where CO_2 is removed at a rate of 20.23 µmol kg^{-1} d^{-1} for the DMC experiments.

Comparative methodology and model evaluation: The standard model version has been evaluated against observed ocean biogeochemical properties in Chien et al. (2022). Biogeochemistry in the nested version has not yet been evaluated in a publication so a brief assessment of relevant properties, i.e., those relevant for ocean carbonate chemistry, was made here. This was done by comparing both FOCI configurations against a GLODAP data climatological mean. For these comparisons all model output was regridded to the GLODAP observational grid

using CDO software. For other comparisons between the standard and nested versions, the standard model output was regridded to the nest grid using CDO software.

2.3 Results

2.3.1 Comparison of Baseline Model Carbonate Chemistries

Before evaluating the simulated ocean-based CDR, an understanding of the differences between observations and the baseline (control) standard and nested simulations, as well as between the standard and nested simulations is needed. As shown in Figure 6 both model versions tend to underestimate total alkalinity (TA) in most places. Although there are also some areas where the models simulate too much TA with this being more pronounced in the nested version.

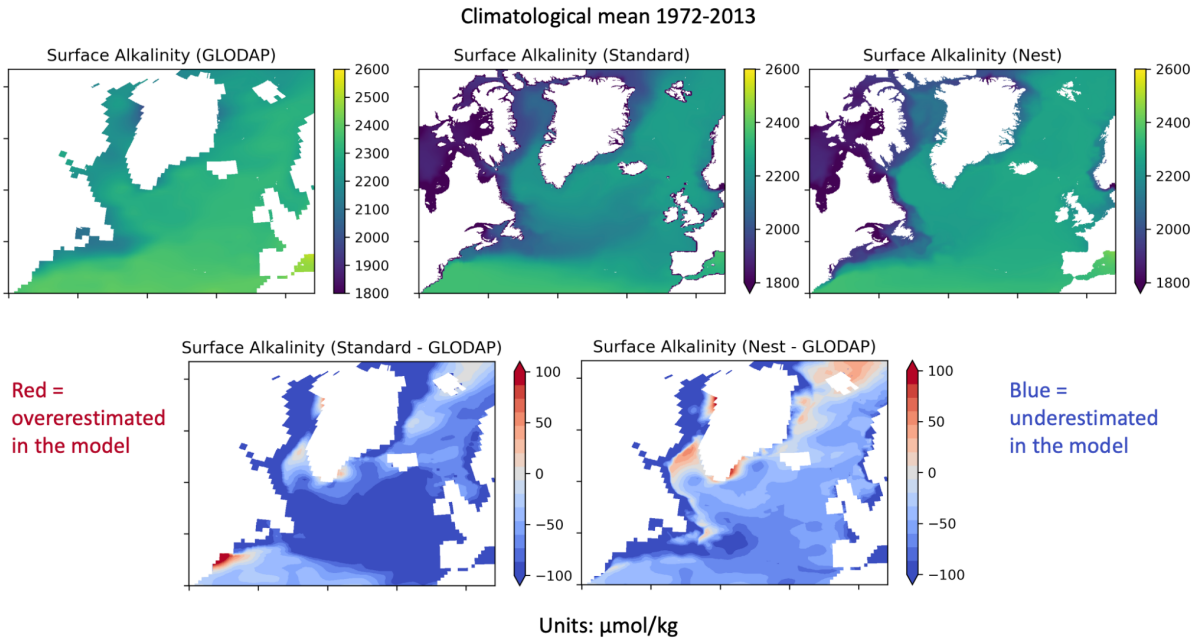

Figure 6. Comparison between observed GLODAP and simulated recent historical total alkalinity with both model versions.

As shown in Figure 7, surface dissolved inorganic carbon (DIC) tends to be too low in the standard version in most places, with the nested version performing somewhat better. Both models also have regions, which are often in similar locations, where DIC is too high.

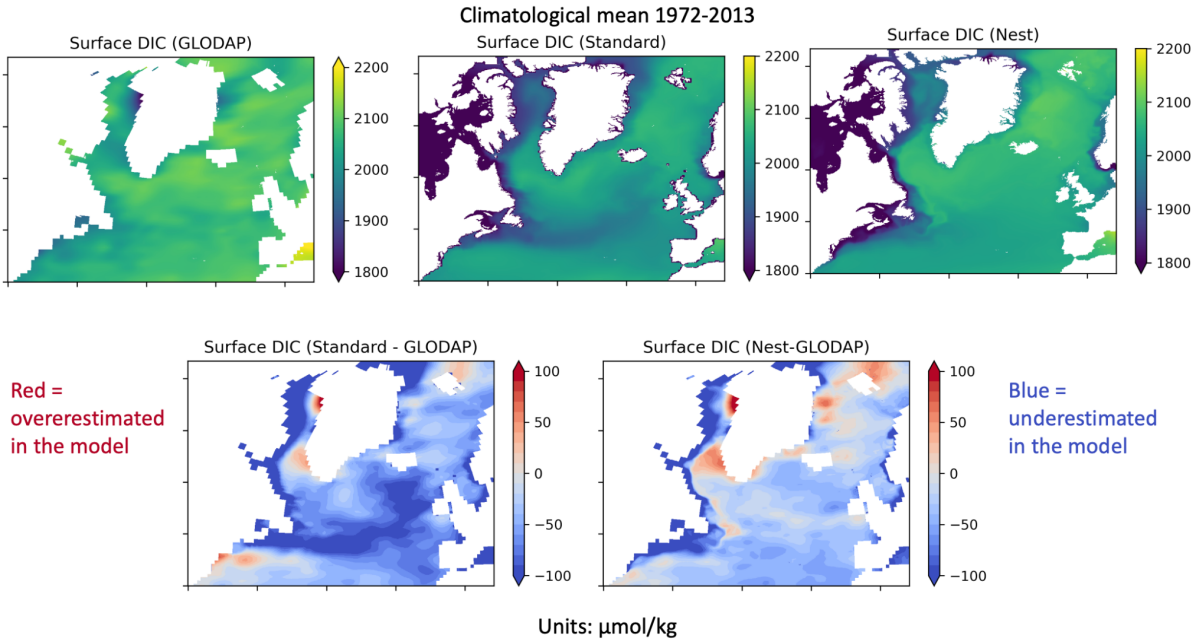

Figure 7. Comparison between observed GLODAP and simulated recent historical dissolved inorganic carbon (DIC) with both model versions.

Overall, the standard version tends to be more biased than the nested version. However, these biases are similar to the biases in other state-of-the-art ESMs (Hinrichs et al., 2023; Planchat et al., 2023) and thus, the model performance can be considered reasonable.

2.3.2 OAE results

As expected with OAE, alkalinity increased substantially in both model configurations when compared to the control simulations (Fig. 8). Although alkalinity is added to coastal European regions, little accumulates there as it is transported and mixed into the Arctic and Labrador Sea regions (Fig. 8 c and d), as well as the Western Atlantic. Some of the alkalinity from OAE is also transported into the Mediterranean Sea. Due to differences in circulation, alkalinity increases from OAE are higher in the Western Atlantic and central Labrador Sea and lower in the Norwegian and Mediterranean Seas, as well as off the Iberian Peninsula, with the nested configuration when compared to the standard one (Fig. 8 e). Some notable differences related to resolution and bathymetry can also be seen along the coast and at physical features such as shelf breaks.

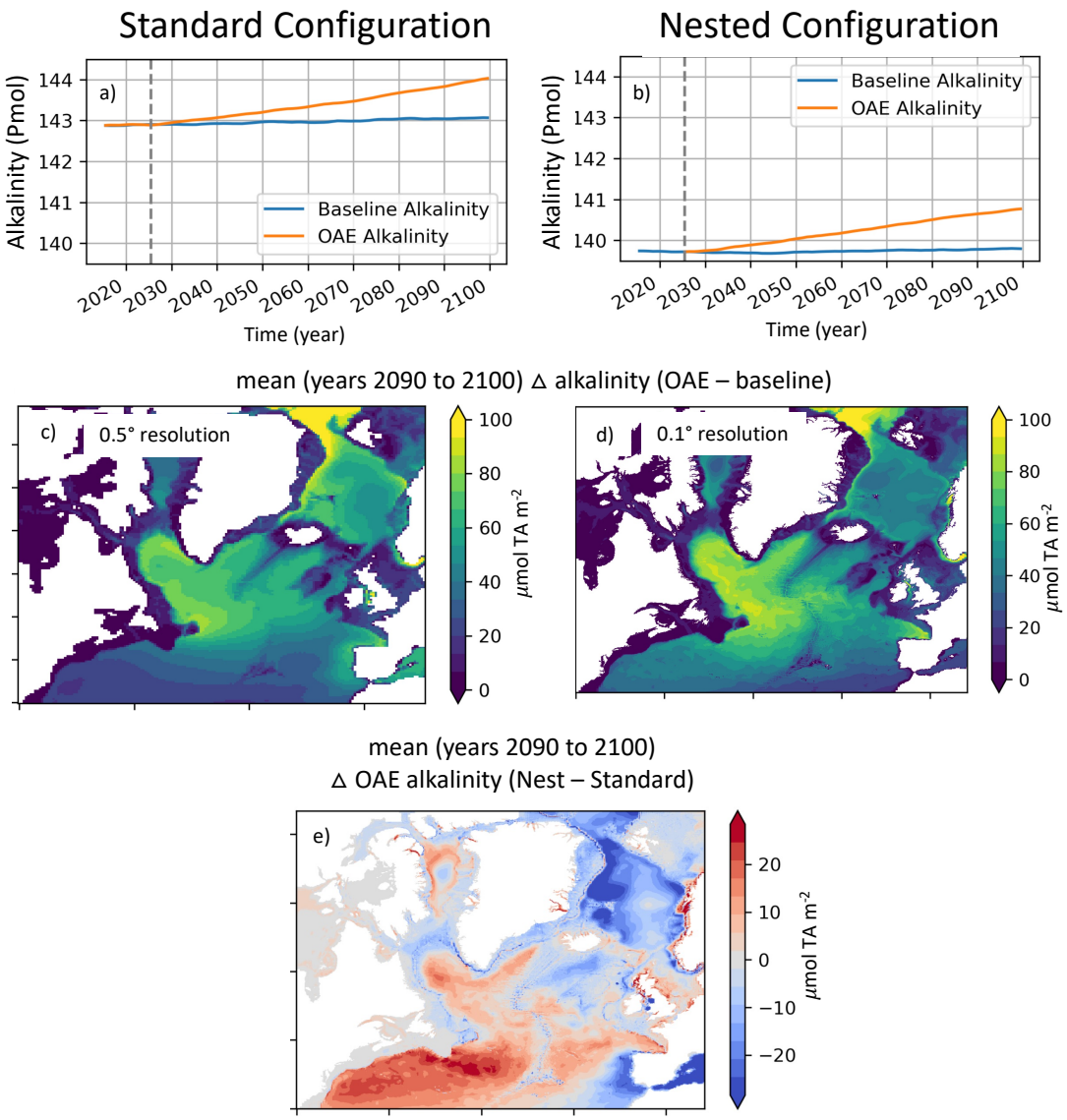

Figure 8. Simulated mean (years 2090 to 2100) total alkalinity (TA) increases with and without the nest (Nest and Standard respectively) for alkalinity added along the EU coast. Differences in the distribution of alkalinity towards the end of the simulations are shown in e, where the standard model output has been regridded to that of the nest for comparison.

In response to simulated OAE the ocean takes up more carbon (Figs. 9 and 10). The overall trend in CO_2 uptake in all runs follows the SSP5-3.4-OS scenario CO_2 emissions forcing (Fig. 3), although with a lagged response. For example, even though the scenario has negative CO_2 emissions that start around 2070, the ocean carbon flux only periodically turns negative (loss of ocean C) in a few runs by the year 2100.

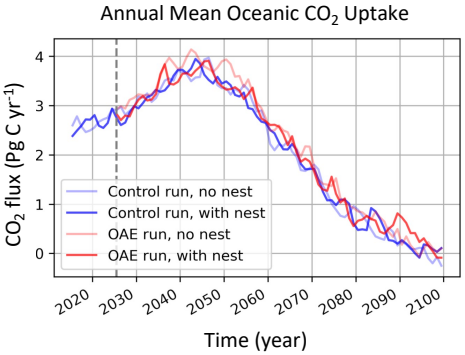

Figure 9. Simulated global annual mean oceanic CO_2 uptake (Pg C yr^{-1}) for both model configurations with and without (referred to as control run or baseline) OAE.

With both model configurations, much of the OAE induced carbon uptake occurs outside of the region where alkalinity is increased (Fig. 10). There are also some notable differences due to model resolution. In the nested configuration more carbon is taken up near the UK, Irish, Norwegian, and Icelandic coastlines and less carbon taken up is taken up in the North and Norwegian Seas and off the Iberian Peninsula, when compared to the standard configuration. There are also some small differences in carbon uptake south of Greenland and in the Western Atlantic, however, these are likely not due to OAE.

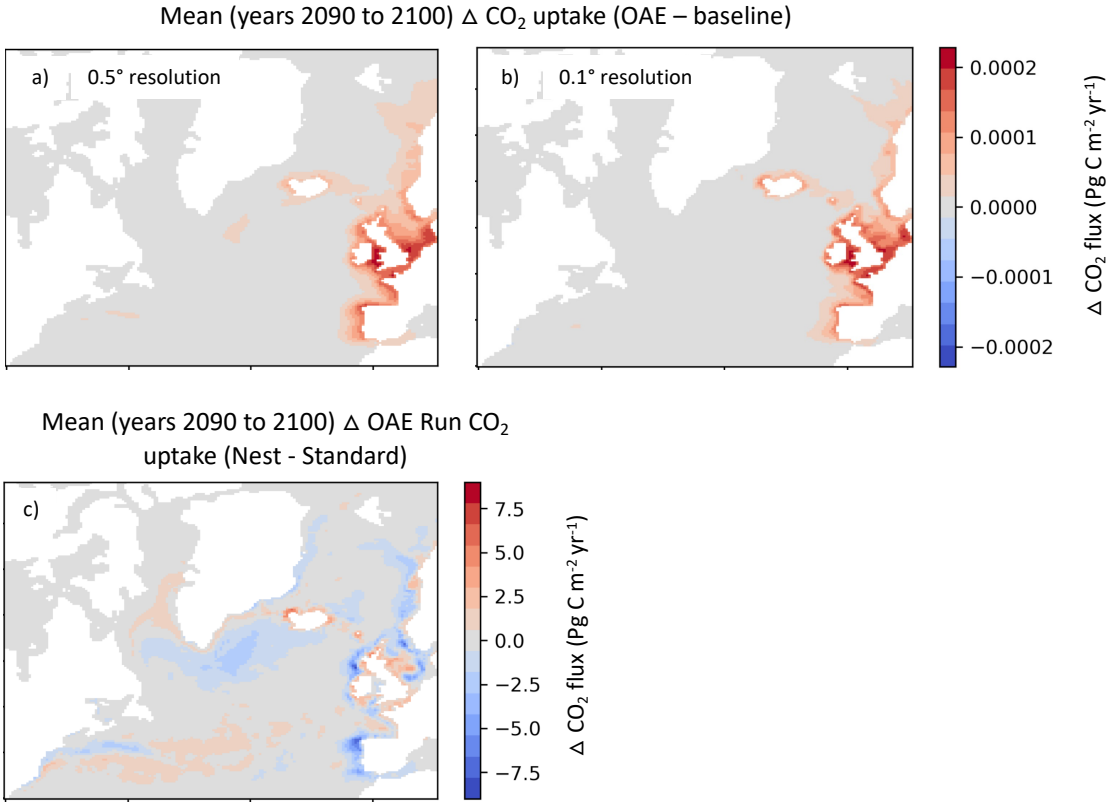

Figure 10. Simulated mean (years 2090 to 2100) changes in ocean CO_2 uptake due to OAE for the standard (a) and nested (b) model configurations. Differences (Nest – Standard) between the model versions are shown in (c). All data is shown on the standard grid.

Although OAE causes more carbon to be taken up and stored in both configurations, when compared to the baseline simulations, less carbon is sequestered and stored with the nested one (Fig. 11). By the year 2100 simulated OAE has resulted in more than twice as much carbon being stored in the ocean with the standard configuration, when compared to the nested one. The distribution of OAE induced DIC sequestration and storage is also different. With the nested configuration DIC is higher in the Western Atlantic and lower in the Norwegian and Mediterranean Seas, as well as off the Iberian Peninsula, when compared to the standard configuration. As with alkalinity, there are some notable differences in DIC related to resolution and bathymetry along the coast and at physical features such as shelf breaks.

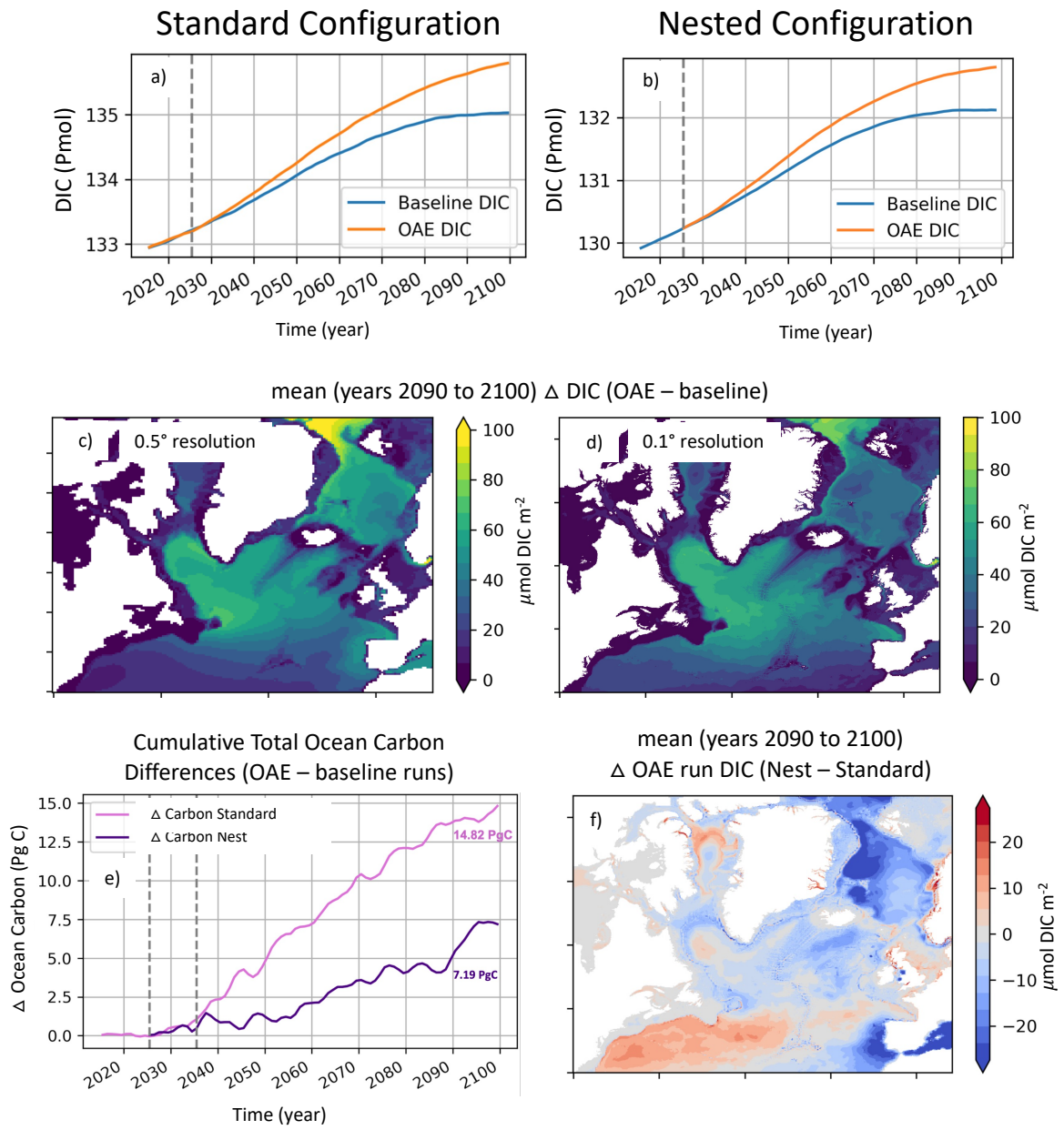

Figure 11. Simulated changes in oceanic dissolved inorganic carbon (DIC) with and without the nest (Nest and Standard respectively) for the baseline(control) and OEA experiments (a and b) and the difference between the OAE and baseline experiments (e), i.e., carbon sequestered and stored due to OAE. In (e) the cumulative difference in DIC at the year 2100 is noted. In (c) and (d) mean (years 2090 to 2100) water column inventory DIC changes are shown, with differences between the model configurations shown in (f), where the standard model output has been regridded to that of the nest for comparison.

Although simulated OAE was of the same magnitude and in nearly the same locations with the two model configurations, except for notable bathymetric / topographic differences, the efficacy of OAE as a means to increase ocean carbon storage and reduce atmospheric CO_2 is very different when calculated as the change in oceanic DIC per change in total alkalinity (Fig. 12). Efficacy with the standard model configuration is much higher, averaging around 0.7 moles of DIC stored per mol of alkalinity added, when compared to the nested version which averages around 0.3 moles of DIC stored per mol of alkalinity added. This suggests that on these timescales, full equilibration (air-sea gas exchange) of the OAE water has not occurred in the nest and that the better resolved physical circulation, e.g., mixing and subduction, at 0.1° resolution is limiting how long OAE waters stay in contact with the surface.

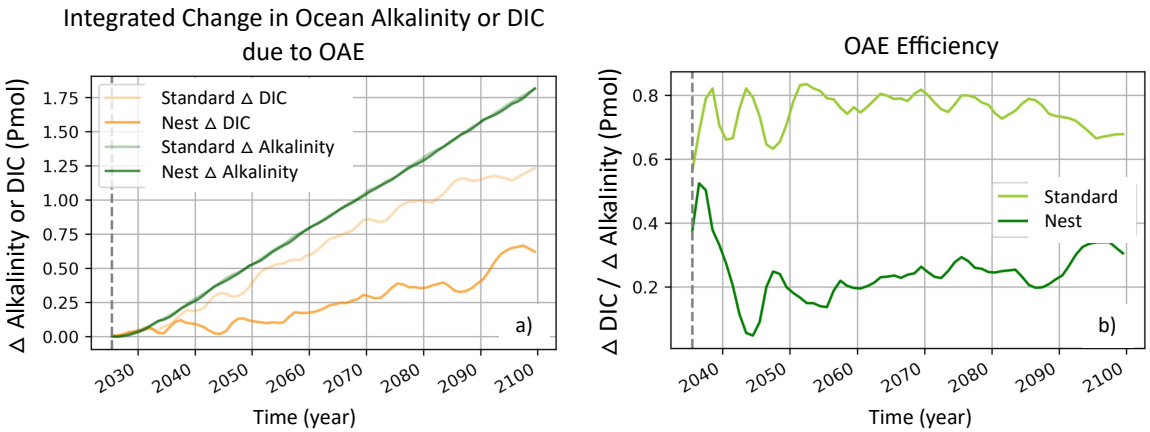

Figure 12. The global total change in alkalinity or DIC (a) and the efficacy of OAE at increasing oceanic carbon storage (b) when calculated as the global change in DIC per change in alkalinity. All differences (deltas) are relative to the baseline (control) run simulations for both model resolution configurations. In (b) years during the OAE ramp-up phase are not shown due to internal model variability that produce a large range of efficiencies.

Few side effects are able to be diagnosed with the models as there is no direct impact of OAE on biology that has been parameterized in the biogeochemical model component, i.e., simulated carbonate chemistry has no influence to plankton growth or other dynamics. In theory, only indirect climatic impacts are able to be resolved, however, these were too small to be detected with this level of regional OAE (not shown). That is there is no detectable change in plankton dynamics due to OAE induced climatic changes, although there are small differences due to model variability. However, as it is possible that changes in carbonate chemistry could have an impact on biological processes, we show how pH changes with OAE (Fig. 13). OAE does increase pH by a substantial amount with changes over 0.6 pH units, when compared to the baseline (control) simulations. Much of the OAE induced change in pH occurs outside of the region where alkalinity is increased. There are also some notable differences due to model resolution (Fig. 13 c). In the nested configuration the change in pH is higher near the UK, Irish, Norwegian, and Icelandic coastlines and lower in the North and Norwegian Seas and off the Iberian Peninsula, when compared to the standard configuration. There are also some small differences in pH near Greenland, Hudson Bay, and in the Western Atlantic, however, these are likely not due to OAE.

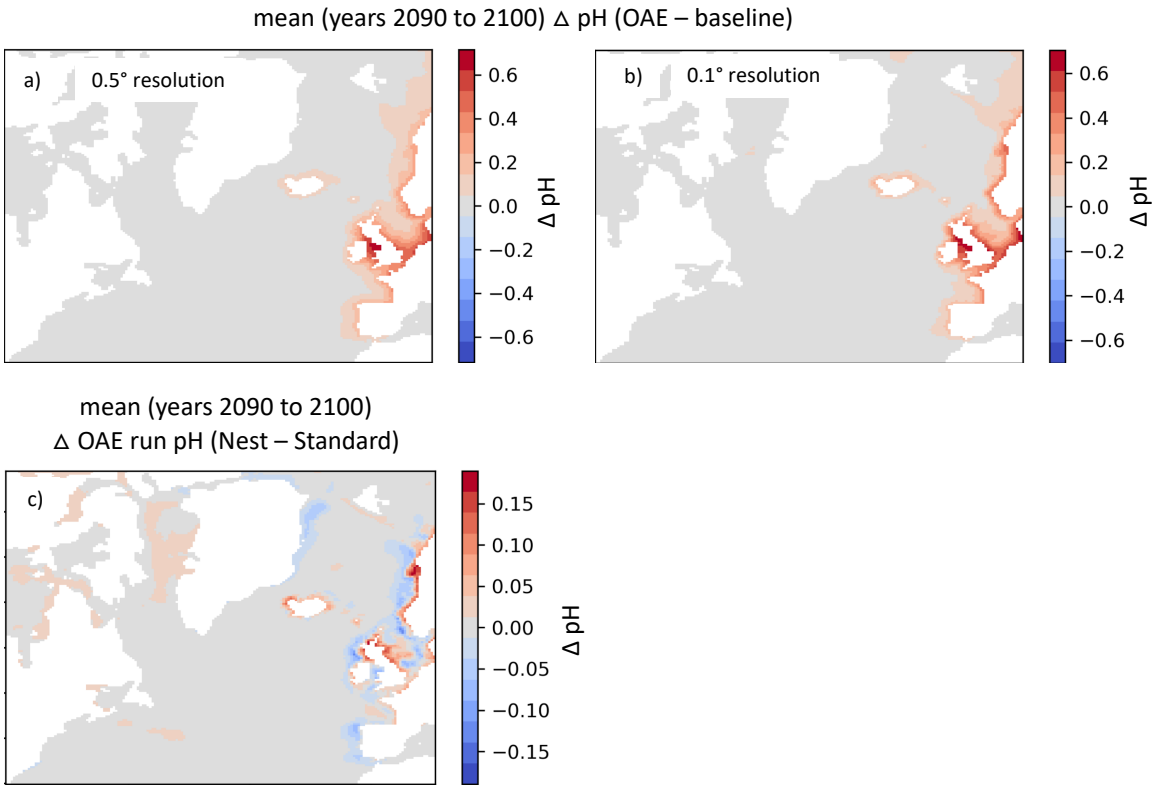

Figure 13. Simulated mean (years 2090 to 2100) changes in ocean pH for the standard (a) and nested (b) model configurations during OAE. Differences (Nest – Standard) between the model versions are shown in (c).

2.3.3 Direct Marine Capture of CO_2

The simulated direct marine capture (DMC) of CO_2 (with assumed permanent storage), results in clear changes in DIC at and downstream from the sites of removal (Figs. 14 and 15). The change in DIC is larger at the North Sea site, although also more variable, with a maximum decrease of ~650 μmol Kg^{-1} with the nested model configuration. At the Spanish site there are some clear differences between model configurations with the standard version DIC change being about 100 μmol Kg^{-1} higher (less over all DIC) than with the nested configuration. The variability in DIC at the North Sea site is too high to see clear, persistent difference between model configurations. With both model configurations low DIC waters can be seen many tens of kilometers beyond the removal site after one month, indicating that air-sea gas exchange compensation for the removal and mixing, take time to restore DIC to that of surrounding waters. This is further illustrated in Fig. 14 where, at the DMC site after cessation, DIC has not returned within one month to that of the baseline runs in most simulations. When low DIC waters are transported outside of the DMC site, the nested and standard configurations show differences in circulation as these waters sometimes go in the opposite direction when the runs are compared (Fig. 15).

The removal of DIC from seawater causes air-sea gas exchange of CO_2 to increase, resulting in enhanced ocean C uptake, as the atmosphere and ocean re-equilibrate (Figs. 16 and 17). The CO_2 flux is highly variable, but overall, much higher in the DMC simulations, when compared to the baseline runs. As with DIC, there are some clear, persistent difference between model configurations at the Spanish DMC site (Fig. 17 d) with the nested configuration having a lower enhancement of CO_2 uptake than the standard configuration. At the North Sea site persistent differences between model configurations are not clear, except perhaps after the cessation of DMC,

when the nest has consistently higher CO_2 uptake (Fig. 17 c). As low DIC waters are transported away from the sites differently with the two model configurations (Fig. 15), due to circulation differences, CO_2 uptake enhancement, which can happen many 10s of kilometers from the DMC site, also tends to be different (Fig. 16; other dates not shown).

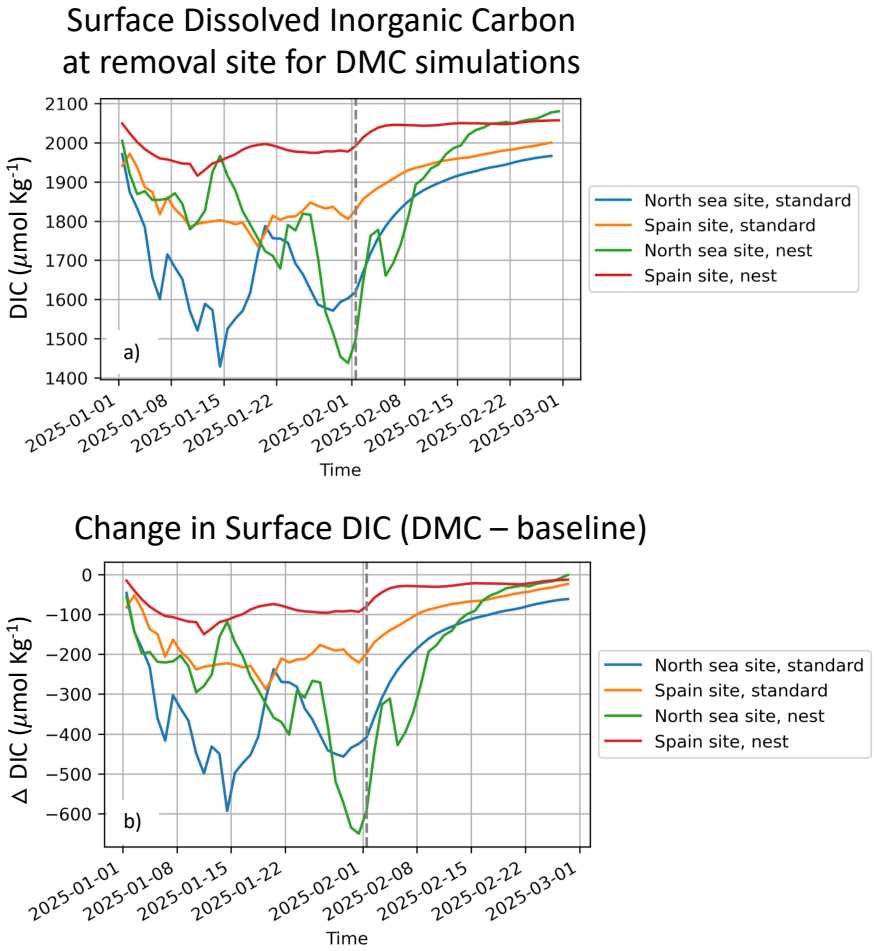

Figure 14. Surface grid cell dissolved inorganic carbon (DIC) and the change in DIC (DMC – baseline run) at the direct marine capture (DMC) sites in the North Sea and off the coast of Spain. Only DMC simulations are shown. The vertical grey dashed line indicates the date at which DMC was stopped in the DMC experiments.

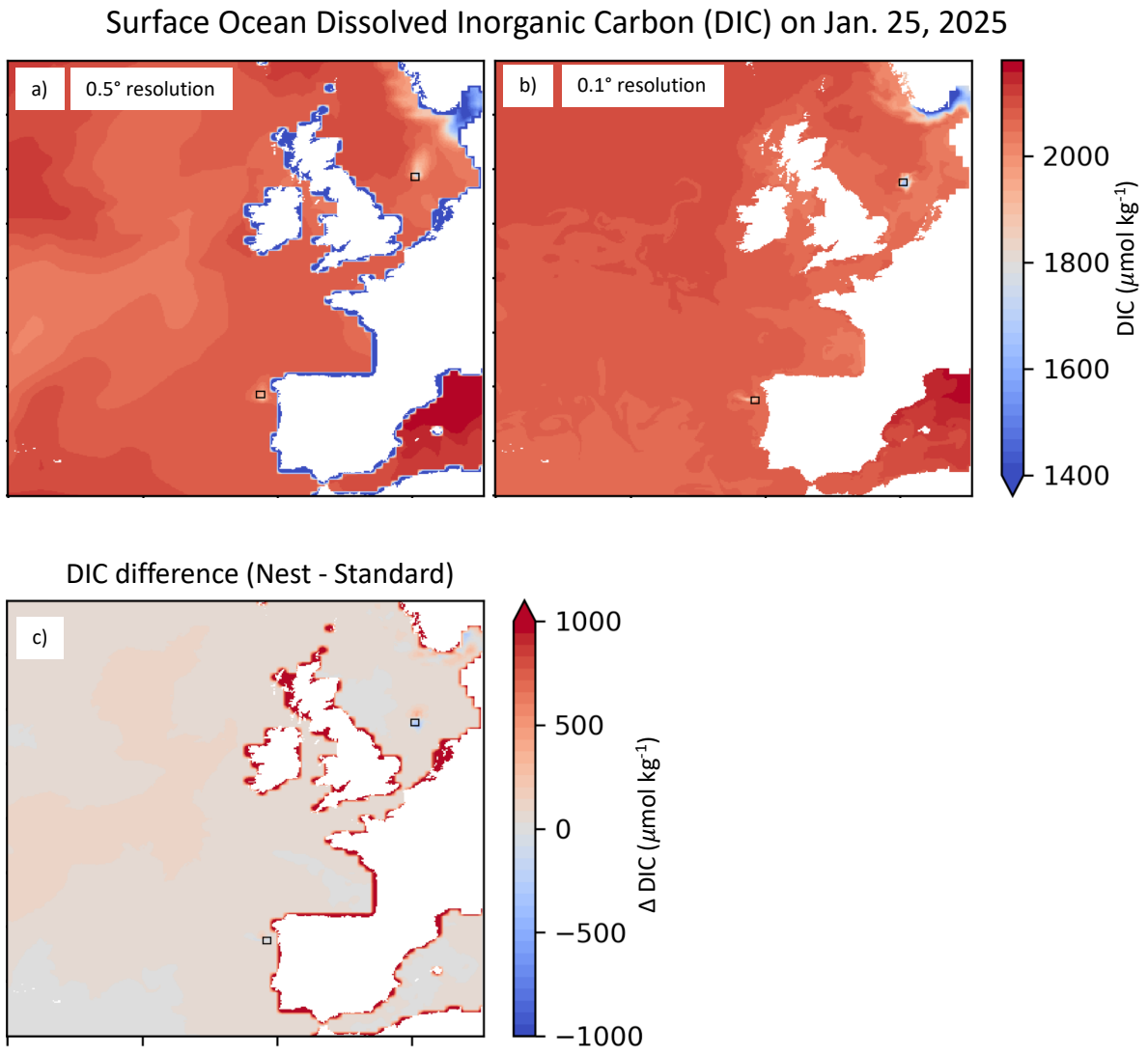

Figure 15. Simulated surface ocean DIC for the standard (a) and nested (b) model configurations on Jan. 25, 2025 during DMC. Differences (Nest – Standard) between the model versions are shown in (c). The extreme values near the coastline in (a) and (c) are the result of re-gridding the coarse resolution (0.5°) output onto the high-resolution grid for comparison and represent areas where there is no output due to the lower resolution.

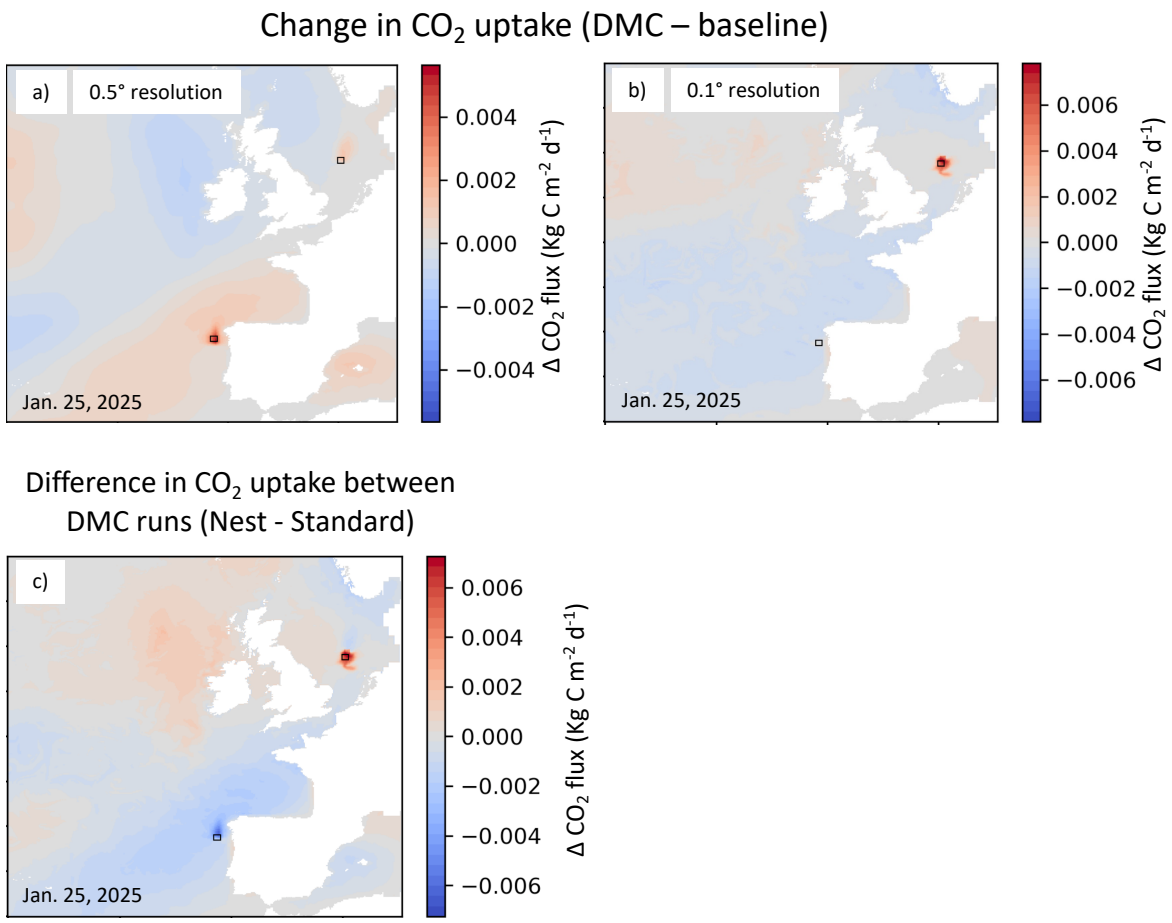

Figure 16. Snapshot of the daily mean change in the surface ocean CO_2 flux for the standard (a) and nested (b) configurations, relative to their baseline (control) simulations, after 25 days of Direct Marine Capture (DMC) of DIC. The CO_2 flux difference between the nested and standard DMC experiments is shown in (c) where the standard model output has been re-gridded to that of the nest for comparison.

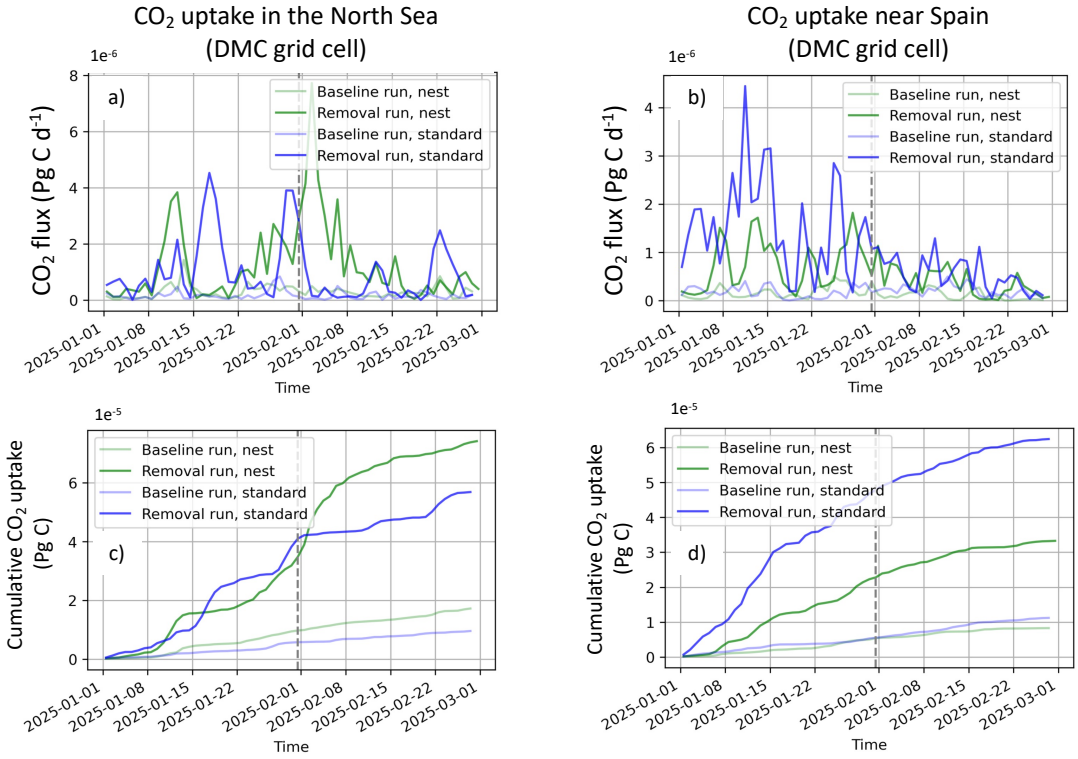

Figure 17. Simulated CO_2 fluxes at the direct marine capture (DMC) sites in the North Sea (a and c) and off the coast of Spain (b and d) with both model resolution configurations and for baseline and DMC experiments. Cumulative carbon uptake,

calculated from the CO_2 flux data is shown in (c) and (d). The vertical grey dashed line indicates the date at which DMC was stopped in the DMC experiments.

Impacts of DMC on carbonate chemistry are pronounced near the sites of DIC removal, as exemplified by the changes in pH (Figs. 18 and 19). pH changes were largest in the North Sea and extended many 10s of kms beyond the site of removal. However, the North Sea site also had higher variability with clear early differences between model resolution versions that were not as pronounced by late January. Whereas there were persistent differences at the Spanish site, with the standard version showing a pH change ~0.2 higher than in the nested version. Differences in the simulated circulation at different resolutions were also very evident with downstream impacts going in the opposite direction in the North Sea. Overall, these changes followed the patterns seen in the DIC and CO_2 flux uptake changes (Fig. 15 and 16), which both influence pH, but in opposite directions with DIC removal increasing pH and ocean CO_2 uptake reducing pH. Here it is obvious that the DIC removal has the largest influence on pH as it consistently increases. After DMC stops pH begins to recover, i.e., decrease from high values, but at the removal sites, most simulations had not fully recovered after a month. As there is no effect of carbonate chemistry changes on plankton growth or other dynamics in this model, no biological impacts were evident (not shown). The magnitude of DMC was also too small to have a detectable impact on atmospheric CO_2 or the climate.

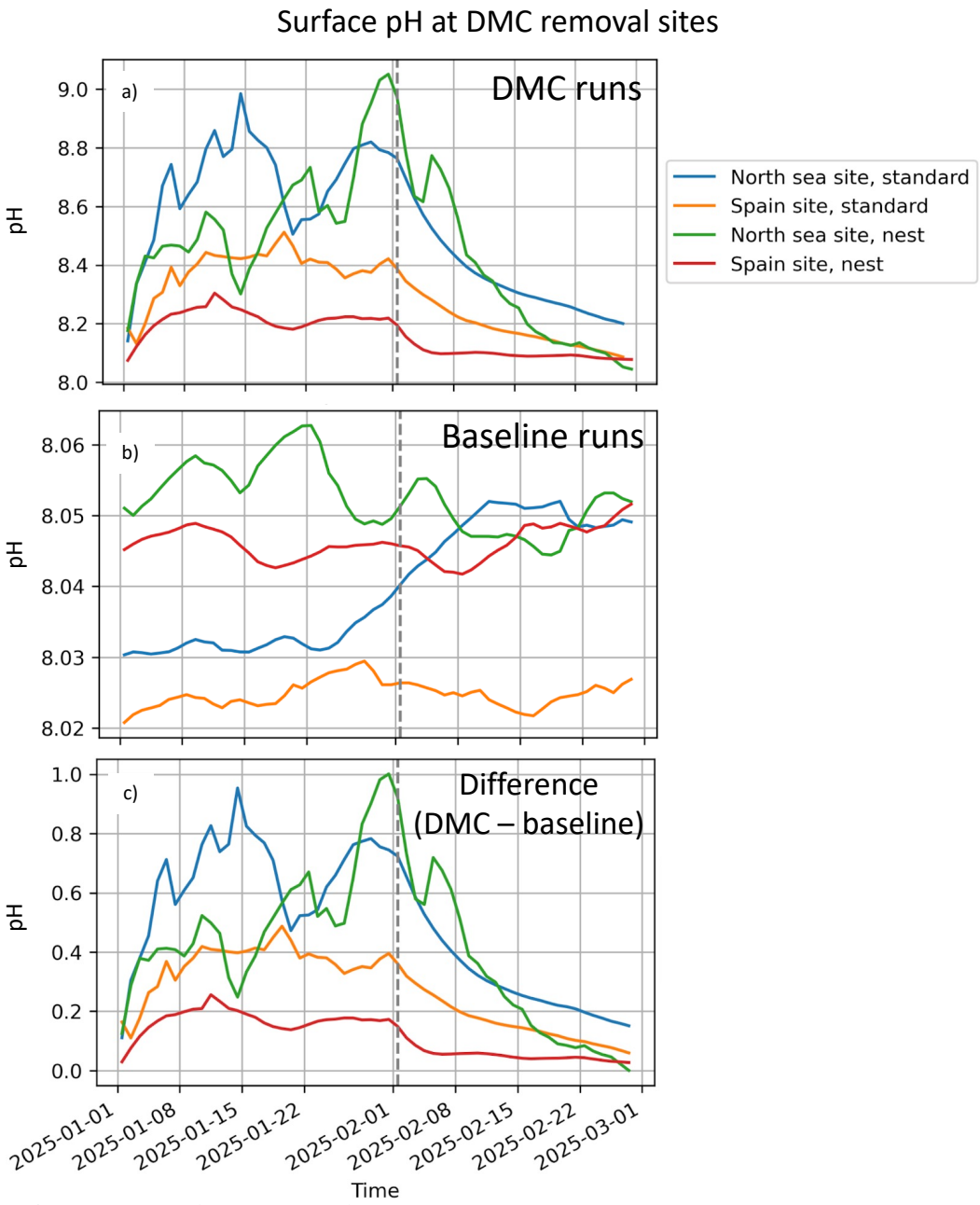

Figure 18. Surface ocean pH at the DMC removal sites.

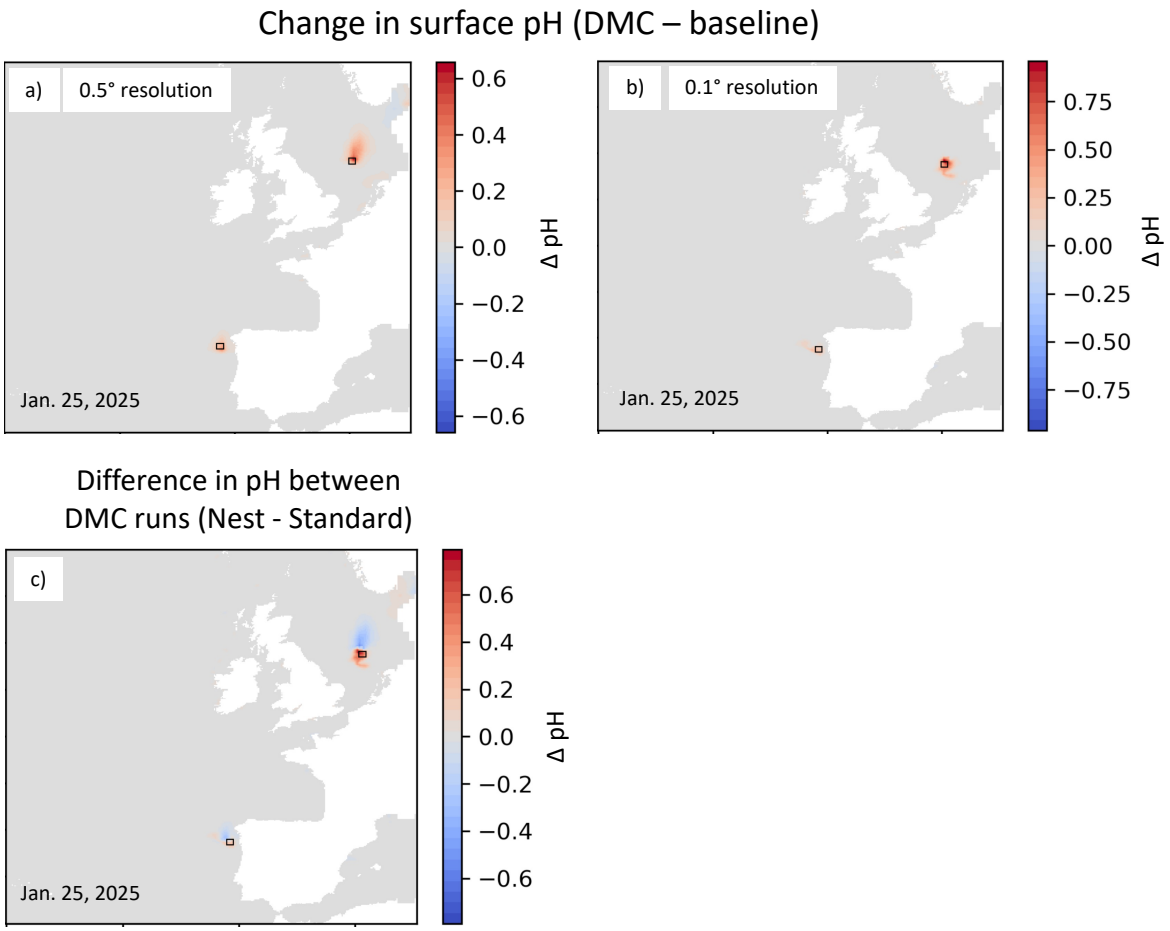

Figure 19. Snapshot of the daily mean change in surface ocean pH for the standard (a) and nested (b) configurations, relative to their baseline (control) simulations, after 25 days of Direct Marine Capture (DMC) of DIC. The pH difference between the nested and standard DMC experiments is shown in (c) where the standard model output has been re-gridded to that of the nest for comparison.

2.4 Discussion

2.4.1 OAE experiments

Idealized modelling studies have shown that increasing the alkalinity of seawater could potentially remove large amounts of CO_2 from the atmosphere (up to 450 ppm) and keep it there even if the additions were stopped (Burt et al., 2021; Feng et al., 2017; González & Ilyina, 2016; Ilyina et al., 2013; Keller et al., 2014; Köhler et al., 2013). In these studies, the models had resolution of 1° or greater and thus, had to parameterize physical ocean processes like mesoscale eddies. While these parameterizations allow the models to perform reasonably when simulating ocean biogeochemistry, the climate system, and climate change (Bopp et al., 2013; Eby et al., 2013; IPCC, 2013, 2021), they also suggested that OAE could be done with a fairly high efficiency with values often reported to range from 0.7 to 0.9 moles of DIC stored per mol of alkalinity added. Such efficiencies are near the theoretical average physio-chemical efficiency under typical surface conditions of around ~0.8 moles of DIC stored per mol of alkalinity added (Renforth et al., 2013; Tyka et al., 2022) and suggest that the alkalized water fully equilibrates on short time scales. However, recent OAE simulations with a higher resolution regional model at 1/16° Butenschön et al., (2021) have suggested that efficiencies are generally lower (between 0.2 and 0.5 moles of DIC stored per mol of alkalinity) when ocean physics are better resolved. Something that the study

largely attribute to incomplete equilibration before some of the alkalized water is transported into the ocean interior. But model resolution alone may not fully explain differences in efficacy as Wang et al., (2023) found very high OAE efficiencies even with a high resolution model (10 kms). They attribute this to unique regional ocean physics that allowed for long equilibration times of the alkalized waters. He and Tyka (2023), who used a mid-resolution model of 1/3°, have also reported that efficiencies vary regionally as a result of differences in coastal circulation. Thus, both model resolution and the location of OAE appear to be important for determining OAE carbon sequestration efficacy.

As far as we are aware, no study has yet tried to directly evaluate the importance of model resolution on simulated OAE as we have done. Our results show that when ocean physics are better resolved by increasing model resolution (see Martin and Biastoch (2023)), OAE efficiencies for a relatively large coastal European deployment tend to be lower. This suggests that to determine optimal deployment locations and when models are used for monitoring, reporting, and verification (MRV) purposes, high resolution simulations are likely needed to determine realistic OAE efficacies. Alternatively, an improvement of the physical parameterizations could be considered for coarser resolution model OAE simulations. Although this may not be adequate for coastal OAE, where it makes sense to have higher resolutions that best represent the bathymetry. Of course, it is also important to validate the model against observations and make sure that physics are properly represented. Based on our study we cannot determine what the best resolution is in all cases as this likely depends on the characteristics of the site and the manner in which OAE is simulated. Regions with more complex bathymetries, currents, and tides, will need better resolved physics than in areas that are not as physically dynamic.

The biogeochemical component of the model is not able to simulate many potential side effects of OAE because only changes in total alkalinity are parameterized when modeling OAE. Furthermore, there is also no parameterized relationship between simulated carbonate chemistry and the planktonic components of the model. However, we have shown that changes in carbonate chemistry, such as pH, are different with the model resolutions. As with OAE efficiency, a better resolution/representation of physical dynamics is likely important for robustly simulating side effects.

2.4.2 DMC experiments

Direct marine capture (DMC) of CO_2 from seawater is an immature technology (Aleta et al., 2023; Digdaya et al., 2020; Lannoy et al., 2017) that has been proven in laboratory studies and is undergoing pilot studies, but as far as we are aware has not been simulated with Earth system models. Therefore, little is known about how the ocean carbon cycle will respond to the removal of carbon. In theory, after CO_2 is removed by the process and water returned with a lower pCO_2 this should cause the ocean to take up more carbon, thereby sequestering additional carbon. As estimates of the magnitude of carbon that could be removed by DMC are limited, our idealized study was designed to remove a large fraction (30%) of DIC per day from the surface ocean at two different study sites in the hopes of detecting clear signals from DMC. These sites in the North Sea and off the Spanish coast were chosen to contrast a shallow, well mixed area (in winter), with a deeper, upwelling region. Our results show pronounced impacts of DMC on DIC and the ocean carbon flux, both at the sites of removal and many tens of kilometers beyond it. Carbonate chemistry parameters such as pH were also subsequently impacted by DMC. After DMC cessation, the DMC induced changes persisted for longer than a month in most of our simulations, suggesting that longer-term impacts are possible.

Differences in simulated DMC due to model resolution were clear at the Spanish site, where less additional carbon was taken up with the nest (Fig. 17 d), but less so at the North Sea site. Although, for non-local (downstream) effects at both sites, differences in circulation were evident as low DIC waters were often transported in opposite directions with the two model versions. Together these results suggests that model resolution is important for simulating DMC, but more work needs to be done to confirm this.

Overall, our results suggests that while DMC can remove carbon from seawater, if done at a large scale, impacts may not remain localized. Our results also suggest that effects may persist for some time (months), even if the approach is stopped. While this study gives us hints of what may happen with DMC, many more simulations should be done to better quantify its efficacy (via additional carbon uptake) and impacts. Simulations of DMC at different magnitudes, durations, and in additional locations are need. We also suggest conducting longer runs after the termination of DMC to better quantify how long side effects may last. In our particular case, longer simulations would also be useful to see if the DMC signal becomes more pronounced during summer when the mixed layer shallows (in the North Sea) or when upwelling is relaxed off the Spanish coast.

2.4.3 General caveats of these studies

While the OAE and DMC studies do suggest that model resolution matters, there are some caveats that must be mentioned. First, is the coarser atmospheric grid, which is at 1.8°, and thus, requires that air-sea CO_2 flux calculations be averaged when calculating the flux between the mismatched atmospheric and ocean grids. As the air-sea flux is calculated on the atmospheric side this could have an impact on simulated fluxes. Ideally, studies such as ours would have the same oceanic and atmospheric grid resolutions. Second, the model has high internal variability, something common in fully coupled ESMs, that can make detecting a signal difficult or cause one to question any single realization. Ensemble simulations should therefore be done to ensure the robustness of the OAE and DMC results. Third, many side effects are difficult to evaluate as there is no parameterized relationship between simulated carbonate chemistry and the planktonic components of the model. While some models do include such parameterizations (Seifert et al., 2022), data to parameterize these effects are scarce and thus, most models do not include them. Finally, large scale OAE and DMC field experiments have not been done so there are no observations to compare our results to. Thus, we cannot validate how well the model simulates either CDR approach.

3. Conclusion and Outlook

Overall, we have shown that model resolution does appear to matter when simulating OAE and DMC. For OAE, parameterization of physical processes in the coarse resolution version of our model appear to overestimate how long alkalized waters stay in contact with the atmosphere and where they are transported. This results in large differences in OAE efficacy with almost twice as much carbon sequestered when the model resolution is coarse. For the DMC simulations, at one site there were clear differences in the compensating CO_2 flux induced by DIC removal, while at the other site variability was high and differences were difficult to determine. However, at both DMC sites there were clear differences in circulation, and thus on downstream biogeochemistry. We suggest that well resolving ocean physics may be necessary to best calculate unequilibrated OAE and DMC efficacies and side effects. These results should be confirmed using other models and with different resolutions. Hopefully optimal resolutions can be found for different OAE and

DMC applications that balance the need to well resolve ocean physics against the computational expense of running high resolution model configurations.

To address some of the issues and further, unanswered questions in this study, we have already begun running ensemble simulations. We have also completed additional OAE runs to evaluate how regional efficiencies vary, as well as how point source deployments differ from the more widespread OAE which was simulated here. Furthermore, we have started to investigate how pulsed (at different times of the year and of different magnitudes and duration) OAE deployments differ from continuous ones in terms of efficacy. This work will contribute to determining the best locations and approaches for doing OAE. For DMC, we are also starting to plan more experiments that build upon the results presented here.

4. Data availability

Model output used in this study is available at:
https://data.geomar.de/downloads/20.500.12085/514b741d-48b6-48dd-a087-34858cfa7a20/ssp534os/

Full model output (i.e., variables not used in the analysis above) from these simulations is several terabytes in size and available upon request.

5. References

Aleta, P., Refaie, A., Afshari, M., Hassan, A., & Rahimi, M. (Mim). (2023). Direct Ocean Capture: The Emergence of Electrochemical Processes for Oceanic Carbon Removal. *Energy & Environmental Science*. https://doi.org/10.1039/D3EE01471A

Bopp, L., Resplandy, L., Orr, J. C., Doney, S. C., Dunne, J. P., Gehlen, M., et al. (2013). Multiple stressors of ocean ecosystems in the 21st century: projections with CMIP5 models. *Biogeosciences*, *10*(10), 6225–6245. https://doi.org/10.5194/bg-10-6225-2013

Burt, D. J., Fröb, F., & Ilyina, T. (2021). The Sensitivity of the Marine Carbonate System to Regional Ocean Alkalinity Enhancement. *Frontiers in Climate*, *3*, 68. https://doi.org/10.3389/fclim.2021.624075

Butenschön, M., Lovato, T., Masina, S., Caserini, S., & Grosso, M. (2021). Alkalinization Scenarios in the Mediterranean Sea for Efficient Removal of Atmospheric CO2 and the Mitigation of Ocean Acidification, *3*(614537). Retrieved from https://www.frontiersin.org/articles/10.3389/fclim.2021.614537/full

Chien, C.-T., Durgadoo, J. V., Ehlert, D., Frenger, I., Keller, D. P., Koeve, W., et al. (2022). FOCI-MOPS v1 - Integration of Marine Biogeochemistry within the Flexible Ocean and Climate Infrastructure version 1 (FOCI 1) Earth system model. *Geoscientific Model Development Discussions*, 1–58. https://doi.org/10.5194/gmd-2021-361

Digdaya, I. A., Sullivan, I., Lin, M., Han, L., Cheng, W.-H., Atwater, H. A., & Xiang, C. (2020). A direct coupled electrochemical system for capture and conversion of CO 2 from oceanwater. *Nature Communications*, *11*(1), 4412. https://doi.org/10.1038/s41467-020-18232-y

Eby, M., Weaver, a. J., Alexander, K., Zickfeld, K., Abe-Ouchi, A., Cimatoribus, a. a., et al. (2013). Historical and idealized climate model experiments: an intercomparison of Earth system models of intermediate complexity. *Climate of the Past*, *9*(3), 1111–1140. https://doi.org/10.5194/cp-9-1111-2013

Feng, E. Y., Koeve, W., Keller, D. P., & Oschlies, A. (2017). Model-Based Assessment of the CO 2 Sequestration Potential of Coastal Ocean Alkalinization. *Earth's Future*, *5*(12), 1252–1266. https://doi.org/10.1002/2017EF000659

González, M. F., & Ilyina, T. (2016). Impacts of artificial ocean alkalinization on the carbon cycle and climate in Earth system simulations. *Geophysical Research Letters*, *43*(12), 6493–6502. https://doi.org/10.1002/2016GL068576

Haarsma, R. J., Roberts, M., Vidale, P. L., Senior, C. A., Bellucci, A., Bao, Q., et al. (2016). High Resolution Model Intercomparison Project (HighResMIP). *Geoscientific Model Development Discussions*, (April), 1–35. https://doi.org/10.5194/gmd-2016-66

He, J., & Tyka, M. D. (2023). Limits and CO_2 equilibration of near-coast alkalinity enhancement. *Biogeosciences*, *20*(1), 27–43. https://doi.org/10.5194/bg-20-27-2023

Hinrichs, C., Köhler, P., Völker, C., & Hauck, J. (2023). Alkalinity biases in CMIP6 Earth System Models and implications for simulated CO2 drawdown via artificial alkalinity enhancement. *Biogeosciences Discussions*, 1–21. https://doi.org/10.5194/bg-2023-26

Ilyina, T., Wolf-Gladrow, D., Munhoven, G., & Heinze, C. (2013). Assessing the potential of calcium-based artificial ocean alkalinization to mitigate rising atmospheric CO 2 and ocean acidification. *Geophysical Research Letters*, *40*(22), 5909–5914. https://doi.org/10.1002/2013GL057981

IPCC. (2013). *Climate Change 2013: The Physical Science Basis. Contribution of Working Group I to the Fifth Assessment Report of the Intergovernmental Panel on Climate Change*.

IPCC. (2021). *Climate Change 2021: The Physical Science Basis. Contribution of Working Group I to the Sixth Assessment Report of the Intergovernmental Panel on Climate Change* (IPCC).

Jones, C. D., Arora, V., Friedlingstein, P., Bopp, L., Brovkin, V., Dunne, J., et al. (2016). The C4MIP experimental protocol for CMIP6. *Geoscientific Model Development*, (1), 1–52. https://doi.org/10.5194/gmd-2016-36

Keller, D. P., Feng, E. Y., & Oschlies, A. (2014). Potential climate engineering effectiveness and side effects during a high carbon dioxide-emission scenario. *Nature Communications*, *5*, 1–11. https://doi.org/10.1038/ncomms4304

Keller, D. P., Lenton, A., Scott, V., Vaughan, N. E., Bauer, N., Ji, D., et al. (2018). The Carbon Dioxide Removal Model Intercomparison Project (CDRMIP): rationale and experimental protocol for CMIP6. *Geoscientific Model Development*, *11*(3), 1133–1160. https://doi.org/10.5194/gmd-11-1133-2018

Köhler, P., Abrams, J. F., Völker, C., Hauck, J., & Wolf-Gladrow, D. A. (2013). Geoengineering impact of open ocean dissolution of olivine on atmospheric CO2 , surface ocean pH and marine biology. *Environmental Research Letters*, *8*(1), 14009.

Kriest, I, & Oschlies, A. (2015). MOPS-1 . 0 : modelling the regulation of the global oceanic nitrogen budget by marine biogeochemical processes, 1945–2010. https://doi.org/10.5194/gmdd-8-1945-2015

Kriest, Iris, Helmholtz-zentrum, G., Kiel, O., & Weg, D. (2017). Calibration of a simple and a complex model of global marine biogeochemistry, 4965–4984.

Lannoy, C. D., Eisaman, M. D., Jose, A., Karnitz, S. D., Devaul, R. W., Hannun, K., & Rivest, J. L. B. (2017). International Journal of Greenhouse Gas Control Indirect ocean capture of atmospheric CO 2 : Part I . Prototype of a negative emissions technology. *International Journal of Greenhouse Gas Control*, (May), 0–1. https://doi.org/10.1016/j.ijggc.2017.10.007

Madec, G. (2016). NEMO Ocean Engine. Note du Pole de modelisation de l'Institut Pierre-Simon Laplace (IPSL), France.

Martin, T., & Biastoch, A. (2023). On the ocean's response to enhanced Greenland runoff in model experiments: relevance of mesoscale dynamics and atmospheric coupling. *Ocean Science*, *19*(1), 141–167. https://doi.org/10.5194/os-19-141-2023

Matthes, K., Biastoch, A., Wahl, S., Harlaß, J., Martin, T., Brücher, T., et al. (2020). The Flexible Ocean and Climate Infrastructure version 1 (FOCI1): mean state and variability. *Geoscientific Model Development*, *13*(6), 2533–2568. https://doi.org/10.5194/gmd-13-2533-2020

National Academy of Sciences, Engineering, and Medicine. (2021). *A Research Strategy for Ocean-based Carbon Dioxide Removal and Sequestration*. Washington, D.C.: The National Academies Press.

O'Neill, B. C., Tebaldi, C., Van Vuuren, D. P., Eyring, V., Friedlingstein, P., Hurtt, G., et al. (2016). The Scenario Model Intercomparison Project (ScenarioMIP) for CMIP6. *Geoscientific Model Development*, *9*(9), 3461–3482. https://doi.org/10.5194/gmd-9-3461-2016

Orr, J. C., & Epitalon, J.-M. (2015). Improved routines to model the ocean carbonate system: mocsy 2.0. *Geoscientific Model Development*, *8*(3), 485–499. https://doi.org/10.5194/gmd-8-485-2015

Orr, James C., Najjar, R. G., Aumont, O., Bopp, L., Bullister, J. L., Danabasoglu, G., et al. (2017). Biogeochemical protocols and diagnostics for the CMIP6 Ocean Model Intercomparison Project (OMIP). *Geoscientific Model Development*, *10*(6), 2169–2199. https://doi.org/10.5194/gmd-10-2169-2017

Planchat, A., Kwiatkowski, L., Bopp, L., Torres, O., Christian, J. R., Butenschön, M., et al. (2023). The representation of alkalinity and the carbonate pump from CMIP5 to CMIP6 Earth system models and implications for the carbon cycle. *Biogeosciences*, *20*(7), 1195–1257. https://doi.org/10.5194/bg-20-1195-2023

Renforth, P., Jenkins, B. G., & Kruger, T. (2013). Engineering challenges of ocean liming. *Energy*, *60*, 442–452. https://doi.org/10.1016/j.energy.2013.08.006

Rodgers, K. B., Schwinger, J., Fassbender, A. J., Landschützer, P., Yamaguchi, R., Frenzel, H., et al. (2023). Seasonal Variability of the Surface Ocean Carbon Cycle: A Synthesis. *Global Biogeochemical Cycles*, *37*(9), e2023GB007798. https://doi.org/10.1029/2023GB007798

Schmittner, A., Oschlies, A., Matthews, H. D., & Galbraith, E. D. (2008). Future changes in climate, ocean circulation, ecosystems, and biogeochemical cycling simulated for a business-as-usual CO2 emission scenario until year 4000 AD. *Global Biogeochemical Cycles*, *22*, GB1013. https://doi.org/10.1029/2007GB002953

Schneck, R., Reick, C. H., & Raddatz, T. (2013). Land contribution to natural CO2 variability on time scales of centuries. *Journal of Advances in Modeling Earth Systems*, *5*(2), 354–365. https://doi.org/10.1002/jame.20029

Seifert, M., Nissen, C., Rost, B., & Hauck, J. (2022). Cascading effects augment the direct impact of CO2 on phytoplankton growth in a biogeochemical model. *Elementa: Science of the Anthropocene*, *10*(1), 00104. https://doi.org/10.1525/elementa.2021.00104

Tyka, M. D., Arsdale, C. V., & Platt, J. C. (2022). CO2 capture by pumping surface acidity to the deep ocean. *Energy & Environmental Science*, *15*(2), 786–798. https://doi.org/10.1039/D1EE01532J

Wang, H., Pilcher, D. J., Kearney, K. A., Cross, J. N., Shugart, O. M., Eisaman, M. D., & Carter, B. R. (2023). Simulated Impact of Ocean Alkalinity Enhancement on Atmospheric CO2 Removal in the Bering Sea. *Earth's Future*, *11*(1), e2022EF002816. https://doi.org/10.1029/2022EF002816